SPATIAL ANALYSIS OF TREE SPECIES BEFORE FOREST FIRES

A. Novo[1*], H. González-Jorge[2], J. Martínez-Sánchez[1], J. Balado[1]

[1] CINTECX, Universidade de Vigo, GeoTECH group, Campus Universitario de Vigo, As Lagoas, Marcosende 36310, Vigo, Spain (annovo, joaquin.martinez, jbalado)@uvigo.es
[2] Universidade de Vigo, Engineering Physics Group, Campus Universitario de Ourense, 32004, Ourense, Spain- higiniog@uvigo.es

KEY WORDS: Mapping, Forest fires, Remote Sensing, Satellite images, Sentinel-2, GIS analysis, Tree species.

ABSTRACT:

Spain is included in the top five European countries with the highest number of wildfires. The occurrence and magnitude of forest fires involves aspects of a very diverse nature, from those of a socio-economic, climatic, or physiographic nature, to those concerning fuel or the availability and quantity of resources and means of extinction. The distribution of wildfires in Galicia is not random and that fire occurrence may depend on ownership conflicts also a spatial dependence between productive or non-productive area exists. Satellite data play a major role in providing knowledge about fires by delivering rapid information to map fire-damaged areas precisely and promptly. In addition, the availability of large-scale data and the high temporal resolution offered by the Sentinel-2 satellite enables to classify and determine the land cover changes with high accuracy. This study describes a methodology to detect burned areas and analyse the Land Cover and Land Use (LCLU) classes present in these areas during the period of 5 years (2016-2021) by Sentinel-2 images. The training areas were obtained by photointerpretation and the image classification was performed using the Random Forest algorithm which shows an overall accuracy range between 80-85%. The methodology concluded that Lobios and Muiños were the most affected municipalities by wildfires. Additionally, the spatial analysis determined that the Deciduous Forest mainly composed by *Quercus sp.* were the most affected in 2017 followed by Coniferous Forest mainly composed by *Pinus sp.*in 2016. Although, Scrub and Rock are the classes more affected for wildfire during 2016-2020 period.

1. INTRODUCTION

Forest disturbance due to fires being a major challenge for forest management in several ecosystems is because of loss of life and infrastructure, emissions of greenhouse gases, degradation, soil erosion, and the destruction of species, biomass, and biodiversity (Chandra and Bhardwaj, 2015; Pribadi and Kurata, 2017). The South of Europe – Portugal, Spain, France, Italy and Greece – have been seriously affected both economically and environmentally by these kinds of human-ignited wildfires (chAs-AMil et al., 2010). In terms of damage to Natural 2000 sites, the most affected country in 2021 was Italy, followed closely by Spain. Both countries account for 45% of the total burnt area in Natura 2000 sites (San-Miguel-Ayanz et al., 2021). According to the provisional statistics compiled by the relevant departments in the autonomous regions, during 2020 there were 19 large forest fires (GIF) a category which includes fires more than 500 hectares. Regarding the incidence of GIF by geographic regions, the Northwest region of Spain (Galicia, Asturias, Cantabria, León and Zamora) experienced not only the highest number of fires but also the region with the greatest burnt area. Concretely the fourth largest fire was located in Cualedro (1036.71 ha burned) (San-Miguel-Ayanz et al., 2021) Galicia region and that belongs to Xurés National park which is the object of study in this research.

The occurrence and magnitude of forest fires involves aspects of a very diverse nature (Cornwell et al., 2015), from those of a socio-economic, climatic, or physiographic nature, to those concerning fuel or the availability and quantity of resources and means of extinction.

* Corresponding author

In Galicia, human-caused fires account for up to 95% of the total annual fires (López-Rodríguez et al., 2021), highlighting the importance of examining in detail the distribution of this type of phenomenon.

The distribution of wildfires in Galicia is not random and that fire occurrence may depend on ownership conflicts also a spatial dependence between productive or non- productive area exists. The determining factor in the occurrence of forest fires could be the economic value of the existing forest mass. Several authors have linked the relevance of forest fires events to changes in land use and landscape management, as well as the introduction of non-native species (Gómez-González et al., 2019; Pausas and Ribeiro, 2013) others authors have cited a greater number of fires after the substitution of native vegetation with allochthonous species (McWethy et al., 2018; Miranda et al., 2017).

Satellite data play a major role in providing knowledge about fires by delivering rapid information to map fire-damaged areas in a precisely and promptly. Optical Remote Sensing tools have proven to be useful in the development of procedures to accurately estimate fire-affected areas and burn severity, in support of forest fire prevention, assessment and monitoring on global, regional, and local scales (Chuvieco, 2009). These techniques have been mainly employed to address three different temporal fire-related phases: pre-fire conditions, burn severity, and post-fire ecosystem responses (Abdollahi et al., 2018; Chu and Guo, 2014).

The Sentinel-2 mission developed and operated by the European Space Agency (ESA) as part of the Copernicus programme of the European Commission (EC) has provided free of charge high-resolution optical imagery since 2015. The Sentinel-2 data are characterized by high spatial resolution (10-20 m, depending on the band) and high temporal frequency (5 days). To map

burnt areas by Sentinel-2 images the most used indexes are: the burned area index (BAIS2) (Filipponi, 2018), the relative differenced normalized burn ratio (RdNBR) (Miller and Thode, 2007), and the relativized burn ratio (RBR) (Parks et al., 2014) which have been developed and compared using pre-fire and post-fire satellite acquisitions (Chuvieco et al., 2018; Giglio et al., 2018; Quintano et al., 2018; Soverel et al., 2010; Stroppiana et al., 2015). However, the NBR was the spectral index which reported the best classification performances (Filipponi, 2019).

The present research study focuses on pre-fire conditions with the scope of identifying the land cover classes of areas affected by wildfires. One of the essential applications for Sentinel-2 data is Land cover and land use (LCLU) (Bruzzone et al., 2017) which have become essential for decision making and management to assess the status of the Earth's surface and fire risk analysis (de Assis Barros et al., 2021). There is a wide range of algorithms that have been used for the classification of LCLU (Lu and Weng, 2007) among the machine learning algorithms, such as Random Forest (RF) (Breiman, 2001), Classification and Regression Trees (Steinberg and Colla, 2009) and Support Vector Machine (Noble, 2006), which has proven to achieve highly accurate and cover and land use classification results (Nery et al., 2016). There are many recent studies on LCLU which use RF classifies and Sentinel-2 images (Feng et al., 2021; Moraes et al., 2021; Waśniewski et al., 2020; Zhang et al., 2021).

The main aim of this work is to identify the LCLU classes present in the burned areas during the period of 5 years (2016-2021) by Sentinel-2 images. Firstly, the NBR index is calculated by satellite images. Secondly, the LCLU in the pre-fire images are classified and mapped by RF machine learning method. Finally, the relation between the distribution of burned areas and the LCLU classes are statistically analysed. In particular, the main contributions of this study are summarized as:

a) Detection of wildfires for the period 2016-2021.
b) Determination of the training inputs for each year of study.
c) Classification of images for 2016-2021 period in classes.
d) Analysis of classes (Coniferous Forest, Scrub, Rock, Grassland and pastureland, Water, Mixed Forest and Deciduous Forest) in burned areas.

2. MATERIAL AND METHODS

2.1 Area of study

The area of study is located in the northwest of Spain. It belongs to the Natural Park of Baixa Limia Serra do Xurés, which has been catalogued as an Area of Special Conservation (ASC). The object of this study (Figure 1) is an area of 71,287 ha and consists of 9 municipalities which is catalogued as high risk areas and classified at a very high potential risk index (Xunta de Galicia, 2021). The area of study has registered forest fires every year therefore, it is catalogued as an area of high fire activity, with more than 65 fires in the last five years (Xunta de Galicia, 2021). The climatic type which exists in the Baixa Limia is called sub-Mediterranean oceanic temperate, which indicates a certain aridity in summer, this means a large part of vegetation is adapted to dry periods. Under this climatic type, the potentially dominant vegetation in most of the territory is *Quercus pyrenaica* and *Quercus robur*. The main tree species are, *Betula alba, Quercus suber, Arbutus unedo, Pinus sp., Ulex sp., Cytisus scoparius and Erica sp.* These are several endemic plants, including Portugal laurel and *Prunus lusitanica*, a species that colonizes the ravines and other areas that have high humidity. The biogeographical location of Baixa Limia greatly favours the diversity of the flora in this territory.

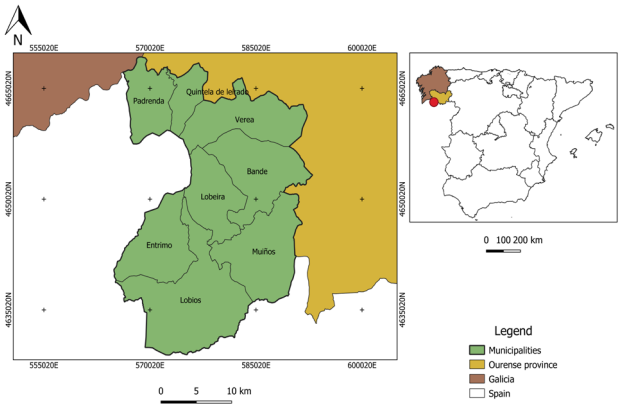

Figure 1. Location of the area of study. The map coordinate system is EPSG:25829 ETRS89/UTM zone 29N.

2.2 Image data acquisition and processing

The data used in this study were form Sentinel-2 images data in years 2016 and 2020. In 2021, there are reports of two small forest fires lower than 0,1 ha which could not be detected by satellite images. The Sentinel-2 satellites are composed of two satellites, with the Sentinel-2A launched in 2015 and Sentinel-B in 2017. Images were downloaded from Copernicus Open Access Hub repository in Level 1C (L1C) with the top of atmosphere (TOA) values and Level 2A (L2A) already corrected to bottom of the atmosphere (BOA) values with Sen2Cor. Orthophotos images that were used for the determination of training inputs were those available in the National Aerial Orthophoto Program (PNOA) ("PNOA," 2017), and also in the Forest Map of Spain (MFE) at a scale of 1:25000 (Gobierno de España, 2014) and the Land use layer of Spanish Land Cover Information System (SIOSE) (CNIG, 2021) ,as well as the expert knowledge.

The conversion of Sentinel-2 images L1C to the physical measure of TOA correction were done using the Dark Object Subtraction (DOS) method (Chavez, 1988), which is an image-based technique. DOS method assumes that non-zero signal values over supposedly zero-value dark shaded pixels are atmospheric scattering signals. The method DOS1 was used in this study by the SNAP software of ESA (Zuhlke et al., 2015). In addition, the plugin Sen2Cor was used for the topography correction on the L1C images. One of the important objectives is to obtain a cloud-free classification because of the influence of cloud cover and summer rainfall, this paper used cloud percent <2% for cloud cover. Table 1 shows the images used in this study, the images were selected based on the forest fires registration, selecting pre-fire and post fire images.

Sensor	Date	Cloud cover (%)
S2A-MSIL1C	22/06/2016	0.26
S2A-MSIL1C	20/09/2016	0.26
S2A-MSIL1C	09/03/2017	0
S2A-MSIL1C	05/04/2017	0
S2A-MSIL2A	31/08/2018	0.20

S2A-MSIL2A	10/10/2018	0.27
S2A-MSILL1C	14/02/2019	1.7
S2A-MSIL2A	26/03/2019	0.33
S2A-MSIL2A	24/02/2020	1.6
S2A-MSIL2A	24/05/2020	0.19

Table 1. Sentinel-2 images downloaded.

2.3 Data processing

The study was developed using QGIS software version 3.16 (QGIS Development Team, 2009) for mapping and spatial analysis. Data processing began by detecting fire affected areas.

NBR is used to identify burned areas and provide a measure of burn severity. It is calculated as a radio between the NIR (Band 8A) and SWIR2 (Band 12) values in traditional fashion. The NIR band is sensitive to vegetation chlorophyll content, while the SWIR2 band is sensitive to soil and vegetation water content providing information on typical conditions that occur after the fire events. NBR for Sentinel-2 images was computed according to the Equation 1.

$$NBR = \frac{B8A - B12}{B8A + B12} \quad (1)$$

where *NBR* = Normalized Burn Ratio
B8A = band NIR (Near Infrared)
B12 = band SWIR (Shortwave Infrared)

Pre-fire, healthy vegetation has very high near-infrared reflectance and low reflectance in the shortwave infrared portion of the spectrum. Recently burned areas on the other hand have relatively low reflectance in the near-infrared and high reflectance in the shortwave infrared band. The burned area shows low values on NBR index while healthy vegetation shows high values on NBR index.

In the following step, the NBR difference (dNBR) (Figure 2) between the pre-fire image and post-fire image, which indicates the severity of the calcination is calculated by Equation 2.

$$dNBR = NBRpre - NBRpost \quad (2)$$

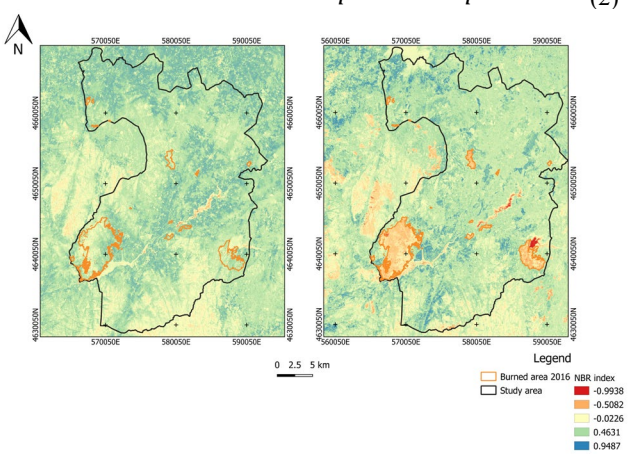

Figure 2. NBR pre-fire (left) and NBR post fire (right) 2016 year.

Next, the Relativized Burn Ratio (RBR) is calculated following the Equation 3.

$$RBR = \frac{dNBR}{NBRpre + 1.001} \quad (3)$$

where *RBR* = Relativized Burn Ratio
dNBR = NBR pre-fire – NBR post-fire

Futhermore, a mask that removes the presence of clouds is generated in the image using the tool Mask Manager using the Green (band 3) and NIR (band 8a) bands which are also created to remove water areas.

Once the water and cloud areas are filtered on the image, the selection of burned areas is carried out, applying a filter of 0.27 value (Key and Benson, 2005) which indicates a low severity (Figure 3). Finally, the forest fires areas selected are vectorized.

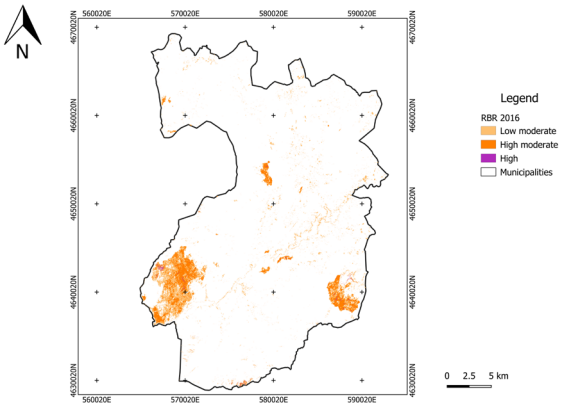

Figure 3. Burn severity levels by RBR 2016 year.

Next stage is the analysis of pre-fire images and the classification in LCLU classes. The methodology proposed consists of three major stages: the pre-processing, the image classification, and the accuracy assessment.

The pre-processing focuses mainly on the consideration of spectral, radiometric and spatial aspects of the images, as these treatments strongly contribute to the quality of the expected results (Butt et al., 2015). First, the radiometric and atmospheric corrections were done based on the image statistics, empirical methods tools, and the radiative transfer model. Second, the spectral bands were combined of each date to form multi-spectral images and the process was input into the Semi-Automatic Classification Plugin (SCP) in QGIS for the classification process.

Next, it is focused on the delineation of training areas. Accurate training plot data are essential for supervised classification. The training area polygons were achieved through photointerpretation and, also by combining image bands with different colour composition. Available layers of LCLU and the expert knowledge were used for photointerpretation, in addition to the field trips carried out for validation. The polygons for each class were distributed homogeneously over the study area, avoiding statistical dependence. Polygons were delineated for each year of study and covering a total of 0.64% of the area of study. Seven classes of LCLU were defined. Table 2 shows the training inputs created for 2016.

Class	Description	Area (ha)
Coniferous forest	Area covered by coniferous trees (Pinus sp.).	41.42
Scrub	Area covered by woody vegetation.	14.64
Deciduous forest	Area covered by deciduous forest (Quercus sp.).	58.85
Mixed forest	Area covered principally of trees, including shrub and bush understoreys.	90.89
Rock	Areas covered by rocks	22.85
Water	Bodies of water.	214.03
Grassland & pastureland	Areas covered by herbaceous vegetation which are used for production.	11.83
Total		454.51

Table 2. Description of LCLU types by year of study.

Then, the image classification was carried out through RF which is a particular machine learning technique, based on the iterative and random creation of decision trees.

Firstly, the input features and classes were defined. RF calculates several random decision trees, based on the number of training samples and the number of trees. Next, to split the trees, a several decision trees randomity using the Gini coefficient. As result, a model based on the decision trees is created and used to classify all the pixels. A pixel is classified according to the majority vote of decision trees. The number of training samples was 5,000 and the number of trees was 500. Secondly, testing the results is a prerequisite in ascertaining the precision or otherwise of the classification performed. In this study, accuracy assessment was done using the SCP in QGIS. A classification error matrix was also formed to articulate the accuracy by tabulating the classified image data and the reference data.

3. RESULTS AND DISCUSSION

Figure 4 shows the results of the burned areas based in the NBR index.

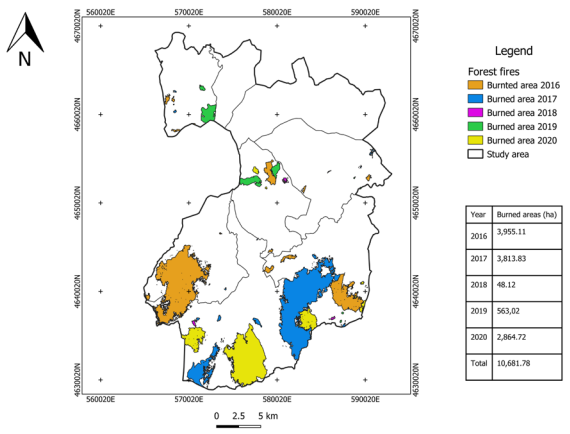

Figure 4. Burned areas mapping.

The total area burned during 2016-2020 represents 15% of the area of study. The largest fires, almost 4,000 ha burned, occurred during 2016 and 2017. Though in 2020 also a large fire took place in the southern of the Natural Park which was located between the fires registered in 2017. Furthermore, the southern region is the most affected owing to fires being recorder in all years of study.

The results of LCLU includ seven classes: Coniferous Forest, Scrub, Water, Rock, Grassland and pastureland, Mixed Forest and Deciduous Forest, for a period of 5 years (2016-2020) and Figure 5 shows the results.

On the one hand, in 2016 and 2017 the Deciduous Forest was the class with largest area covering a total of 2,0754 ha (29% of the study area) and 26,550 ha (37% of the study area) respectively. Nevertheless, since 2018 the area occupied by the Deciduous Forest class was decreasing every year to 2020 with a total of 7,020 ha which represent the 9.85% of the study area. On the other hand, the Scrub class increased of its area from 7,341 ha (10% of the study area) in 2016 to 28,278 ha (40% of the study area) in 2020.

Moreover, there were significant changes in the Coniferous Forest class during the 5 years of study. In 2016 the area covered by Conifers was 15,728 ha (22% of the study area) decreasing to 6,594 ha (9.25% of study area) in 2017. In contrast to the increment in 2018 covering a total of 11,626 ha (16% of the study area). But then the area decreased again to 4,614 ha in 2019 and 4,487 ha (6% of the study area) in 2020.

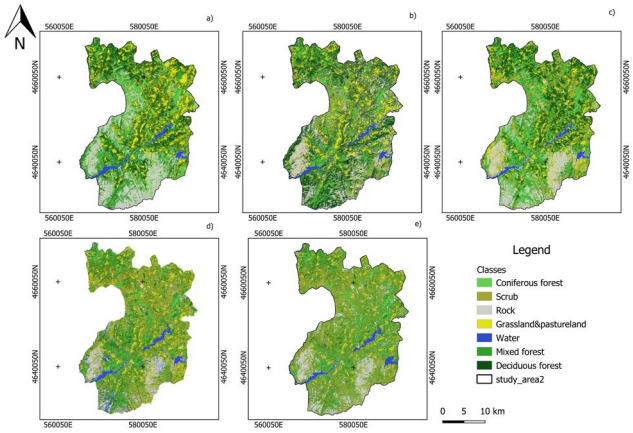

Figure 5. Land use classification maps (a) 2016-year; (b) 2017-year; (c) 2018-year; (d) 2019 year; (e) 2020-year.

The accuracy of the method depends on several factors such as number of training samples, number of land cover classes, the type of the terrain and the pre-processing techniques applied on images. The precision obtained in the classification by RF method ranged 80-85% for the five years of study. The error matrices for the 2016 classification (Table 3.1 and Table 3.2) show that the overall accuracy was 85.6% and the classification kappa was 0.8.

In the Tables 3-7 the numbers correspond with the following classes: 1: Coniferous Forest, 2: Scrub, 3: Rock, 4: Grassland and pastureland, 5: Water, 6: Mixed Forest and 7: Deciduous Forest.

Class	Reference						
	1	2	3	4	5	6	7
1	3971	8	24	0	0	1220	309
2	0	1900	0	6	0	31	56
3	1	0	4092	0	240	135	0
4	0	12	0	695	0	4	2

5	0	0	0	0	21160	0	0
6	100	3	0	0	0	3249	425
7	36	99	1	0	0	1243	3527

Table 3.1 Error matrix (pixel count) 2016 year

	1	2	3	4	5	6	7
PA (%)	97.7	91.8	99.3	99.7	70.3	27.6	90.4
UA (%)	71.7	95.3	91.5	97.4	100	86.0	71.8
OA (%)	85.6						
Kappa	0.8						

Table 3.2. Results obtained for 2016-year classification. PA: Producers Accuracy; UA: User's Accuracy; OA: Total precision and Kappa classification.

The best identified classes in terms of producer's accuracy in 2016 were Coniferous Forest (97.7%), Grassland and pastureland (99.7%) and Rock (99.3%) classes. Furthermore, Mixed Forest was the most misclassified class which was identified as Coniferous Forest (1220 pixels) and Deciduous Forest (1243 pixels).

The error matrix for classification 2017 (Table 4.1 and Table 4.2) shows that the total precision was 80% and the classification kappa was 0.7.

Class	Reference						
	1	2	3	4	5	6	7
1	4194	1	8	0	0	2090	528
2	15	1822	39	288	0	250	71
3	10	4	2029	0	3	90	28
4	0	346	6	2255	0	32	0
5	0	0	0	0	21373	0	0
6	172	20	0	1	12	3468	177
7	115	0	0	0	12	727	2208

Table 4.1 Error matrix (pixel count) 2017 year

	1	2	3	4	5	6	7
PA (%)	86.2	89.8	98.4	81.6	93.7	32.9	85.9
UA (%)	61.4	73.3	93.7	85.4	100	90.0	72.1
OA (%)	80.0						
Kappa	0.7						

Table 4.2. Results obtained for 2017-year classification. PA: Producers Accuracy; UA: User's Accuracy; OA: Total precision and Kappa classification.

On the one hand, the best identified classes in terms of producer's accuracy in 2017, were Rock (98.4%) and Water (93.7%) classes follow by Scrub class (89.8%). On the other hand, Mixed Forest was the least identified class (32.9%) misinterpreted as Coniferous Forest (2090 pixels) class.

The error matrix for classification 2018 (Table 5.1 and Table 5.2) shows that the total precision was 85.2% and the classification kappa was 0.8.

Class	Reference						
	1	2	3	4	5	6	7
1	4322	8	0	0	0	2551	306
2	4	2267	2	7	0	193	117
3	0	0	2281	0	29	0	0
4	0	32	0	1115	0	4	4
5	0	0	15	0	21361	0	0
6	157	30	1	2	5	3388	229
7	23	4	0	44	5	521	803

Table 5.1 Error matrix (pixel count) 2018 year

	1	2	3	4	5	6	7
PA (%)	78.0	98.9	99.5	93.5	96.7	66.4	63.1
UA (%)	60.1	87.5	98.7	96.5	99.9	88.8	57.3
OA (%)	85.2						
K	0.8						

Table 5.2. Results obtained for 2018-year classification. PA: Producers Accuracy; UA: User's Accuracy; OA: Total precision and Kappa classification.

On the one hand, the best identified classes in terms of producer's accuracy in 2018 were Scrub (98.9%) and Rock (99.5%) classes. In addition, only Mixed Forest and Deciduous Forest classes obtained less than 67% of PA. On the other hand, Mixed Forest class was the most misclassified class mistaken for Coniferous Forest (2251 pixels) class.

The error matrix for classification 2019 (Table 6.1 and Table 6.2) shows that the total precision was 82.8% and the classification kappa was 0.7.

Class	Reference						
	1	2	3	4	5	6	7
1	3953	4	0	0	0	2382	287
2	0	2463	6	4	1	180	126
3	0	0	2281	0	27	0	0
4	0	41	0	1119	0	3	9
5	0	0	11	0	21368	0	0
6	139	30	0	0	0	2833	243
7	10	343	1	45	4	484	794

Table 6.1 Error matrix (pixel count) 2019 year

	1	2	3	4	5	6	7
PA (%)	80.5	91.8	98.9	93.9	96.9	63.6	64.5
UA (%)	59.6	88.4	98.8	95.4	99.9	87.3	47.2
OA (%)	82.8						
Kappa	0.7						

Table 6.2. Results obtained for 2019-year classification. PA: Producers Accuracy; UA: User's Accuracy; OA: Total precision and Kappa classification.

The best identified classes in terms of producer's accuracy in 2019, were Rocks (98.9%), Grassland and pastureland (93.9%) and Water (96.9%) classes. The same results than in 2018 were obtained for Mixed and Deciduous Forests with less than 67% in PA. Additionally, Mixed Forest was the most misclassified class mistaken for Coniferous Forest (2382 pixels).

The error matrix for classification 2020 (Table 7.1 and Table 7.2) shows that the total precision was 85.2% and the classification kappa was 0.8.

Class	Reference						
	1	2	3	4	5	6	7
1	3987	4	0	0	0	2299	259
2	0	2750	2	7	0	238	150
3	0	0	2293	0	0	0	1
4	0	44	0	1161	0	2	0
5	0	0	0	0	21400	0	0
6	106	52	4	0	0	2893	289
7	15	31	0	0	0	450	760

Table 7.1 Error matrix (pixel count) 2020 year

	1	2	3	4	5	6	7
PA (%)	81.2	97.8	99.6	97.4	100	70.5	58.4
UA (%)	60.8	87.3	99.9	96.1	100	86.5	60.5
OA (%)	85.2						
Kappa	0.8						

Table 7.2. Results obtained for 2020-year classification. PA: Producers Accuracy; UA: User's Accuracy; OA: Total precision and Kappa classification.

The best identified classes in terms of producer's accuracy in 2020, were Water and Rocks (100% and 99.6% respectively) The classification showed more than 80% of PA in all classes except for Mixed Forest (66.4%) and Deciduous Forest (63.1%) which both are misidentified for Coniferous Forest.

In summary, Water and Rock were the best classified classes, opposite to Mixed Forest class which was mistaken for Coniferous or Deciduous Forest classes.

According to the obtained results, Sentinel-2 images allow for the classification of LCLU of the main classes present in the study area with a high level of accuracy. Deciduous Forest was the class with more presence in the first year of study covering the 37.27% the area of study: However, after five years and when the wildfires occurred the Scrub become the class with more area covering 39.69% the area of study and as consequence the Deciduous Forest decreased 19.2% of its cover area. This aspect is important to consider due to Scrub class consisting of bushes, small multi-stemmed trees, and the like. The more litter there is on the ground to pre-heat above it, the more readily it will ignite, even if the leaves are green. Leaves and twigs will burn quickly and fiercely like grass. If the trunks ignite the fire will be sustained longer and be more intense. Embers from a scrub fire will be larger than those a grass fire and burning debris may also be produced by a scrub fire. Regarding the pyrophytic species belongs to Coniferous Forest class, its area decreased 15.77% in 2016 as consequence of the wildfires.

Figure 6 shows the result of LCLU obtained for each year in the burned areas detected and a detail of a fire which shows the main classes present. Additionally, Figure 7 shows the total of hectares burned for each LCLU classes during each year from period of 2016-2020.

The largest wildfire in the study was in 2016 covering 3952.5 ha. The burned areas were located in both northern and southern of the Natural Park. Although the largest forest fire was located in the southern part, specifically in the municipalities of Entrimo and Lobios. The most area burned were Rock and Coniferous Forest classes with 1,275 ha and 1,220 ha respectively. Also, 661.92 ha of Deciduous Forest and 424.2 ha of Mixed Forest were also burned, particularly in the fire located in the eastern part in Muiños municipality.

In 2017, the wildfires covered a total of 3811,25 ha affecting the municipalities of Lobios and Muiños. The largest burned areas were located in the south part of the Natural Park and Deciduous Forest and Rock were the main classes present in the burned areas, with a total of 1,466 ha and 1,100 ha respectively. Furthermore, 482 ha of Coniferous Forests and 509 ha of Scrub classes also were burned.

In 2018, the wildfires were smaller compared to previous years. The area burned coverd 48.16 ha located in Lobios, Lobeira and Muiños municipalities. The areas were covered by Scrubs (256 ha) and Mixed Forest (120.95 ha).

In 2019, the largest wildfires were located in Lobeira and Padrenda municipalities in the centre and north part of study area. The burned area covered 562.4 ha of which 256.04 ha were covered by Scrub and 120.95 ha for Mixed Forest. Furthermore, the wildfire located in Lobeira municipality occurred one kilometer from the 2018 fire.

In 2020, the wildfires covered 2,862 ha. The burned areas were located in the southern of study area and Lobios was the most affected municipality with 2,700 ha out of 2,862 ha burned. The main class present in the area was Scrub of which 1,211 ha were burned.

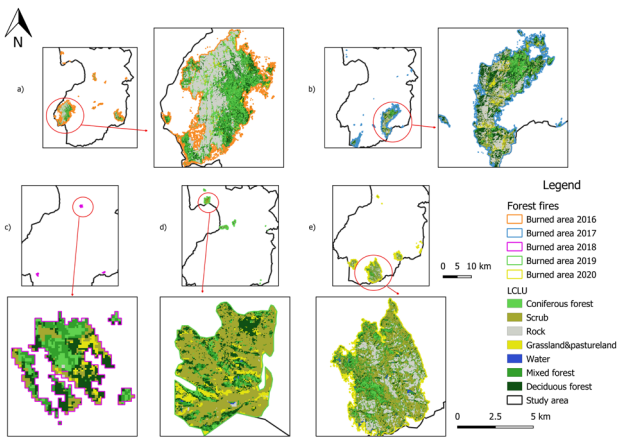

Figure 6. LCLU classes located in the burned areas (a) 2016-year (b) 2017 year; (c) 2018 year; (d) 2019 year; (e) 2020 year.

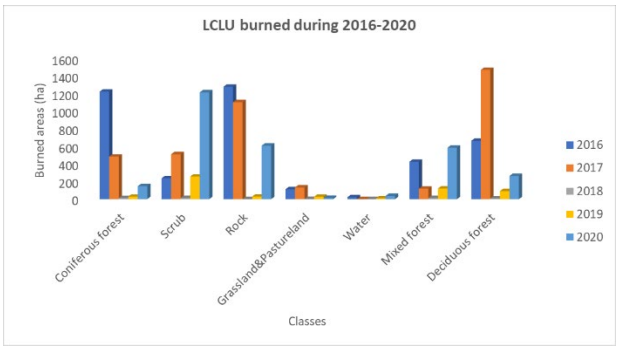

Figure 7. LCLU classes burned during 2016-2020 years in the study area.

Deciduous Forest was the class with more hectares burned in 2017, followed by Rock and Coniferous Forest in 2016. On the

contrary, and without considering the Water class, Grassland and Pastureland were the classes with less hectares burned with the exception of 2017, because of the burned area of Grassland and Pastureland exceeding the Mixed Forest class by 13 ha.

Lobios and Muiños were the most affected municipalities, which have registered wildfires every year of the study except 2017 year in Lobios. In contrast, the municipalities of Quintela de leirado and Verea did not record fires in any year of the study.

4. CONCLUSIONS

The present study shows the potential of Sentinel-2 images to carry out the burned areas detection and LCLU classes classification. The training areas were obtained by photointerpretation and the image classification was performed using the Random Forest algorithm which shows an overall accuracy range between 80-85% for the period of study. The land LCLU classes were identified in the pre-fire images characterizing the vegetation that subsequently burned.

The described methodology concluded that Lobios and Muiños were the most affected municipalities in the Natural Park of Serra do Xures. Additionally, the spatial analysis of tree species determine that the Deciduous Forest mainly composed by *Quercus sp.* were the most affected by forest fires in 2017 followed by Coniferous Forest mainly composed by *Pinus sp.*in 2016. Although, Scrub and Rock are the classes most affected for fire in the period of study.

The results of this study have special interests for forest management. In particular, to generate a database that includes the classes burned in each wildfire and that can be analysed over a longer study period. Moreover, the methodology could be automated in future research.

ACKNOWLEDGEMENTS

A.N. wants to thank University of Vigo through the grant Axudas Predoutorais para a formación de Doutores 2019 (grant number 00VI 131H 6410211) and Project 4Map4Health, selected in the call ERA-Net CHIST-ERA IV (2019), and founded by the State Research Agency of Spain (reference PCI2020-120705-2/AEI/10.13039/501100011033). J.B wants to thank Xunta de Galicia grant numbers ED481B-2019-061 and ED431C 2020/01.

REFERENCES

Abdollahi, M., Islam, T., Gupta, A., Hassan, Q.K., 2018. An Advanced Forest Fire Danger Forecasting System: Integration of Remote Sensing and Historical Sources of Ignition Data. Remote Sens. . https://doi.org/10.3390/rs10060923

Breiman, L., 2001. Random forests. Mach. Learn. 45, 5–32.

Bruzzone, L., Bovolo, F., Paris, C., Solano-Correa, Y.T., Zanetti, M., Fernández-Prieto, D., 2017. Analysis of multitemporal Sentinel-2 images in the framework of the ESA Scientific Exploitation of Operational Missions, in: 2017 9th International Workshop on the Analysis of Multitemporal Remote Sensing Images (MultiTemp). IEEE, pp. 1–4.

Butt, A., Shabbir, R., Ahmad, S.S., Aziz, N., 2015. Land use change mapping and analysis using Remote Sensing and GIS: A case study of Simly watershed, Islamabad, Pakistan. Egypt. J. Remote Sens. Sp. Sci. 18, 251–259.

Chandra, K.K., Bhardwaj, A.K., 2015. Incidence of forest fire in India and its effect on terrestrial ecosystem dynamics, nutrient and microbial status of soil. Int. J. Agric. For. 5, 69–78.

chAs-AMil, M.L., TouzA, J., Prestemon, P., 2010. Spatial distribution of human-caused forest fires in Galicia (NW Spain). Ecol. Environ. 137 247-258 137, 247–258.

Chavez, P.S., 1988. An improved dark-object subtraction technique for atmospheric scattering correction of multispectral data. Remote Sens. Environ. 24, 459–479. https://doi.org/https://doi.org/10.1016/0034-4257(88)90019-3

Chu, T., Guo, X., 2014. An assessment of fire occurrence regime and performance of Canadian fire weather index in south central Siberian boreal region. Nat. Hazards Earth Syst. Sci. Discuss. 2, 4711–4742.

Chuvieco, E., 2009. Earth observation of wildland fires in Mediterranean ecosystems. Springer.

Chuvieco, E., Lizundia-Loiola, J., Pettinari, M.L., Ramo, R., Padilla, M., Tansey, K., Mouillot, F., Laurent, P., Storm, T., Heil, A., 2018. Generation and analysis of a new global burned area product based on MODIS 250 m reflectance bands and thermal anomalies. Earth Syst. Sci. Data 10, 2015–2031.

CNIG, 2021. Centro Nacional de Información Geográfica.

Cornwell, W.K., Elvira, A., van Kempen, L., van Logtestijn, R.S.P., Aptroot, A., Cornelissen, J.H.C., 2015. Flammability across the gymnosperm phylogeny: the importance of litter particle size. New Phytol. 206, 672–681.

de Assis Barros, L., Mendonça, B.A.F. de, Sothe, C., Fernandes Filho, E.I., Elkin, C., 2021. Fire in the Atlantic Rainforest: an analysis of 20 years of fire foci distribution and their social-ecological drivers. Geocarto Int. 1–25.

Feng, X., Li, P., Cheng, T., 2021. Detection of Urban Built-Up Area Change From Sentinel-2 Images Using Multiband Temporal Texture and One-Class Random Forest. IEEE J. Sel. Top. Appl. Earth Obs. Remote Sens. 14, 6974–6986.

Filipponi, F., 2019. Exploitation of sentinel-2 time series to map burned areas at the national level: A case study on the 2017 italy wildfires. Remote Sens. 11, 622.

Filipponi, F., 2018. BAIS2: Burned Area Index for Sentinel-2, in: Multidisciplinary Digital Publishing Institute Proceedings. p. 364.

Giglio, L., Boschetti, L., Roy, D.P., Humber, M.L., Justice, C.O., 2018. The Collection 6 MODIS burned area mapping algorithm and product. Remote Sens. Environ. 217, 72–85.

Gobierno de España, 2014. MFE Galicia [WWW Document]. URL https://www.miteco.gob.es/es/cartografia-y-sig/ide/descargas/biodiversidad/mfe_galicia.aspx (accessed 1.10.22).

Gómez-González, S., González, M.E., Paula, S., Díaz-Hormazábal, I., Lara, A., Delgado-Baquerizo, M., 2019. Temperature and agriculture are largely associated with fire

activity in Central Chile across different temporal periods. For. Ecol. Manage. 433, 535–543.

Key, C.H., Benson, N.C., 2005. Landscape assessment: remote sensing of severity, the normalized burn ratio and ground measure of severity, the composite burn index. FIREMON Fire Eff. Monit. Invent. Syst. Ogden, Utah USDA For. Serv. Rocky Mt. Res. Stn.

López-Rodríguez, G., Rodríguez-Vicente, V., Marey-Pérez, M.F., 2021. Study of Forest Productivity in the Occurrence of Forest Fires in Galicia (Spain). Sustainability 13, 8472.

Lu, D., Weng, Q., 2007. A survey of image classification methods and techniques for improving classification performance. Int. J. Remote Sens. 28, 823–870.

McWethy, D.B., Pauchard, A., García, R.A., Holz, A., González, M.E., Veblen, T.T., Stahl, J., Currey, B., 2018. Landscape drivers of recent fire activity (2001-2017) in south-central Chile. PLoS One 13, e0201195.

Miller, J.D., Thode, A.E., 2007. Quantifying burn severity in a heterogeneous landscape with a relative version of the delta Normalized Burn Ratio (dNBR). Remote Sens. Environ. 109, 66–80. https://doi.org/https://doi.org/10.1016/j.rse.2006.12.006

Miranda, A., Altamirano, A., Cayuela, L., Lara, A., González, M., 2017. Native forest loss in the Chilean biodiversity hotspot: revealing the evidence. Reg. Environ. Chang. 17, 285–297.

Moraes, D., Benevides, P., Costa, H., Moreira, F.D., Caetano, M., 2021. Influence of Sample Size in Land Cover Classification Accuracy Using Random Forest and Sentinel-2 Data in Portugal, in: 2021 IEEE International Geoscience and Remote Sensing Symposium IGARSS. IEEE, pp. 4232–4235.

Nery, T., Sadler, R., Solis-Aulestia, M., White, B., Polyakov, M., Chalak, M., 2016. Comparing supervised algorithms in Land Use and Land Cover classification of a Landsat time-series, in: 2016 IEEE International Geoscience and Remote Sensing Symposium (IGARSS). IEEE, pp. 5165–5168.

Noble, W.S., 2006. What is a support vector machine? Nat. Biotechnol. 24, 1565–1567.

Parks, S.A., Dillon, G.K., Miller, C., 2014. A New Metric for Quantifying Burn Severity: The Relativized Burn Ratio. Remote Sens. . https://doi.org/10.3390/rs6031827

Pausas, J.G., Ribeiro, E., 2013. The global fire–productivity relationship. Glob. Ecol. Biogeogr. 22, 728–736.

PNOA [WWW Document], 2017. URL https://pnoa.ign.es/ (accessed 11.22.21).

Pribadi, A., Kurata, G., 2017. Greenhouse gas and air pollutant emissions from land and forest fire in Indonesia during 2015 based on satellite data, in: IOP Conference Series: Earth and Environmental Science. IOP publishing, p. 12060.

QGIS Development Team, 2009. QGIS Geographic Information System, Open Source Geospatial Foundation Project. 2009. [WWW Document].

Quintano, C., Fernández-Manso, A., Fernández-Manso, O., 2018. Combination of Landsat and Sentinel-2 MSI data for initial assessing of burn severity. Int. J. Appl. earth Obs. Geoinf. 64, 221–225.

San-Miguel-Ayanz, J., Durrant, T., Boca, R., Maianti, P., Liberta, G., Artes-Vivancos, T., Oom, D., Branco, A., De Rigo, D., Ferrari, D., 2021. Forest Fires in Europe, Middle East and North Africa 2020, EUR 30862 EN.

Soverel, N.O., Perrakis, D.D.B., Coops, N.C., 2010. Estimating burn severity from Landsat dNBR and RdNBR indices across western Canada. Remote Sens. Environ. 114, 1896–1909.

Steinberg, D., Colla, P., 2009. CART: classification and regression trees. top ten algorithms data Min. 9, 179.

Stroppiana, D., Azar, R., Calò, F., Pepe, A., Imperatore, P., Boschetti, M., Silva, J., Brivio, P.A., Lanari, R., 2015. Integration of optical and SAR data for burned area mapping in Mediterranean Regions. Remote Sens. 7, 1320–1345.

Waśniewski, A., Hościło, A., Zagajewski, B., Moukétou-Tarazewicz, D., 2020. Assessment of sentinel-2 satellite images and random forest classifier for rainforest mapping in gabon. Forests 11, 941.

Xunta de Galicia, 2021. Pladiga [WWW Document]. URL https://mediorural.xunta.gal/gl/temas/defensa-monte/pladiga-2021 (accessed 5.15.22).

Zhang, T., Su, J., Xu, Z., Luo, Y., Li, J., 2021. Sentinel-2 satellite imagery for urban land cover classification by optimized random forest classifier. Appl. Sci. 11, 543.

Zuhlke, M., Fomferra, N., Brockmann, C., Peters, M., Veci, L., Malik, J., Regner, P., 2015. SNAP (sentinel application platform) and the ESA sentinel 3 toolbox, in: Sentinel-3 for Science Workshop. p. 21.